European Conference on Computational Fluid Dynamics
ECCOMAS CFD 2006
P. Wesseling, E. Oñate and J. Périaux (Eds)
© TU Delft, The Netherlands, 2006

LOW DISSIPATIVE METHODS FOR TURBULENT REACTING FLOWS

Bendiks Jan Boersma & Steven van der Hoeven

Delft University of Technology, Department of Mechanical Engineering Mekelweg 2, 2628 CD, The Netherlands
e-mail: b.j.boersma@tudelft.nl
web page: http://www.ahd.tudelft.nl/

Key words: High order methods, Compressible flows, Large Eddy Simulation (LES)

Abstract. *Modeling of scalar transport is an essential point in the simulation of non-premixed turbulent combustion. The fuel and oxidizer streams are, in general, modeled with an equation for the mixture fraction Z. This mixture fraction is a bounded function, i.e. it can never become large than one or smaller than zero. Symmetric central differencing schemes will, in general, produce values larger than one or smaller than zero if the cell Peclet (or cell Reynolds) number is large. Asymmetric (upwind) schemes can be tuned in such a way that the over/under shoot is absent. However, these upwind schemes will always generate a certain amount of numerical diffusion which will interfere with the diffusion given by a turbulence model or sub-grid model. From a modeling point of view numerical diffusion should be minimized. In this paper we propose an accurate numerical method with very low numerical dissipation which can be used for scalar transport and for the compressible Navier-Stokes equations. A drawback of the method is that it is not strictly monotonic.*

1 Introduction

In modern simulation methods of non premixed turbulent combustion, like for instance Large Eddy Simulation (LES) the turbulent mixing is modeled with a sub-grid model. This model must represent the effects that take place on scales smaller than the smallest scale which can be handled by the numerics. In general these models have a dissipative character and in its most simple form these models only alter the viscosity of the flow locally, i.e. eddy viscosity models [8].

Most numerical models also introduce a certain amount of dissipation. The amount of numerical dissipation strongly depends on the type of scheme. Low order central schemes have in general a higher numerical dissipation than high order schemes. Central (symmetric) schemes have in general less dissipation than upwind (asymmetric) schemes. In an actual Large Eddy Simulation the dissipation is always a combination of dissipation

given by the sub-grid model and by the numerics of the LES model. This makes the validation of a sub-grid model complicated because dissipative effects can be contributed to the numerics or the sub-grid model. For the proper validation of the sub-grid model numerical dissipation should be minimized.

In the literature many low dissipative methods are reported, using high order finite differences, compact finite differences and orthogonal polynomials, see for instance Lele (1992), Chu & Fan (1998). The disadvantage of these schemes is that they in general are not very stable. Recently, Boersma (2005), proposed a staggered variant of the scheme compact finite difference scheme as developed by Lele (1992). This new scheme is stable because it has certain symmetry properties, see for instance Verstappen & Veldman (2003). In this paper we will explore the possibility of this scheme for scalar transport in combustion simulations.

Large eddy equations and numerical method

The important length scales in turbulent combustion are in general related to the flame thickness. The flame thickness is related to molecular properties of the fuel and is in general of order 10^{-4} meter. Even with the most powerful supercomputers direct numerical simulation of turbulent combustion in a realistic domain is not feasible. Therefore, any realistic prediction of turbulent combustion should come from a Large Eddy Simulation (LES).

The equations for a Large Eddy Simulation (LES) are obtained from the full Navier-Stokes equations by applying a spatial filter of the following form

$$\overline{\phi}(\mathbf{x},t) = \int_V \phi(\mathbf{x},t) G(\mathbf{x}-\mathbf{x}') d\mathbf{x}'$$

where ϕ is a flow variable, $\mathbf{x}$ is a vector, V is the volume of the fluid, and G a filter kernel. The exact form of G is not important at this stage. In compressible flows often an additional filter or averaging step is performed, the so-called Favre averaging. This averaging is not necessary and it therefore not used in the present paper.

The LES filtered equation for conservation of mass reads:

$$\frac{\partial \overline{\rho}}{\partial t} + \frac{\partial}{\partial x_i}\overline{\rho}\ \overline{u_i} = -\frac{\partial}{\partial x_i}\underbrace{(\overline{\rho u_i} - \overline{\rho}\ \overline{u_i})}_{SGS} \tag{1}$$

In which ρ is the fluids density and u_i the velocity vector. The last term in the equation above is due to the LES filtering, the so-called sub-grid contribution. In a Favre averaged form of the LES equations the subgrid term would be absent in equation (1).

The equation for conservation of momentum reads:

$$\frac{\partial \overline{\rho}\ \overline{u_i}}{\partial t} + \frac{\partial}{\partial x_j}[\overline{\rho}\ \overline{u_i}\ \overline{u_j} + \overline{p}] = \frac{\partial}{\partial x_j}\overline{\tau_{ij}} - \frac{\partial}{\partial x_j}\underbrace{(\overline{\rho u_i u_j} - \overline{\rho}\ \overline{u_i}\ \overline{u_j})}_{SGS} - \frac{\partial}{\partial t}\underbrace{(\overline{\rho u_i} - \overline{\rho}\ \overline{u_i})}_{SGS} \tag{2}$$

In which $\overline{p}$ is the LES filtered pressure and $\overline{\tau}_{ij}$ is the LES filtered viscous stress tensor. Here we will consider Newtonian flows only and the components of the stress tensor can be written as:

$$\tau_{ij} = \mu \left(\frac{\partial u_i}{\partial x_j} + \frac{\partial u_j}{\partial x_i} - \frac{2}{3} \frac{\partial u_k}{\partial x_k} \right)$$

Where μ is the dynamic viscosity of the fluid. Which is in the present study assumed to be constant. The governing equation for the total energy E which is the sum of the internal energy $\rho C_v T$ and the kinetic energy $\rho u_i u_i/2$ reads:

$$\frac{\partial \overline{E}}{\partial t} + \frac{\partial}{\partial x_j}(\overline{u}_j + \overline{p})\overline{E} = \frac{\partial}{\partial x_i}\kappa \frac{\partial \overline{T}}{\partial x_i} + \frac{\partial}{\partial x_j}\overline{u}_i \overline{\tau}_{ij} + h_f \overline{\omega} - \frac{\partial}{\partial x_j} \underbrace{(\overline{u_j E} + \overline{u_j p} - \overline{u}_j \ \overline{E} - \overline{u}_j \overline{p})}_{SGS} \quad (3)$$

In which $E = \rho C_v T + \rho u_i u_i/2$ is the total energy, κ the (constant) thermal diffusion coefficient, ω a source due to the chemical reaction and h_f the formation enthalpy of a chemical reaction. The thermodynamic quantities P, ρ and T are related to each other by the equation of state for an ideal gas

$$\overline{P} = \overline{\rho} R \overline{T}$$

where R is the gas constant.

The transport of the chemical species is derived from a mixture fraction Z. The equation for Z is

$$\frac{\partial \overline{\rho}\ \overline{Z}}{\partial t} + \frac{\partial}{\partial x_j}\overline{\rho}\ \overline{u_j}\ \overline{Z} = \frac{\partial}{\partial x_i}\kappa_j \frac{\partial \overline{Z}}{\partial x_i} - \frac{\partial}{\partial x_j}(\overline{\rho u_i Z} - \overline{\rho}\ \overline{u}_i \overline{Z}) \quad (4)$$

where κ_j is the diffusion coefficient of the chemical mixture.

All the variables in the equations given above are made non-dimensional using the ambient speed of sound c_∞ as reference velocity scale, the ambient density ρ_∞ as reference density, $\rho_\infty c_\infty^2$ as reference pressure, and c_∞^2/C_p as reference temperature. The resulting non-dimensional numbers are the Reynolds, Prandtl, Schmidt and Mach numbers.

The subgrid terms can be modeled in many different ways. Most models use a variant of the gradient hypothesis, i.e. a Smagorinsky type model

$$\overline{\rho u_i u_j} - \overline{\rho}\ \overline{u_i}\ \overline{u_j} = \overline{\rho}(C_s \Delta)^2 |\overline{S}_{ij}| \overline{S}_{ij}$$

where C_s is the so-called Smagorinsky constant, S_{ij} the strain rate in the flow, and Δ the filter width of the LES filter. In some version of the model the Smagorinsky constant is fixed, usually with a value of $C_s \approx 0.1$ in other implementations, the value of C_s is calculated from the flow field itself, the so-called dynamic Smagorinsky model. For the equations for conservation of mass, energy and mixture fraction a similar model can be

derived[1]. The filter width is in general related to the mesh spacing. If we use second order numerics it is logical to assume that subgrid effects given by the LES model are of the same order of the truncation error of the numerical scheme. To minimize the effects of the truncation error we need a discritization with a order which is sufficiently higher than 2.

2 Numerical method

In this section we will briefly describe the numerical method. The equations are discretized on a staggered non-uniform grid in physical space. For the calculation of the derivative of a certain function f on this non-uniform grid the function f is mapped on a uniform grid with help of the following transformation

$$\frac{\partial f}{\partial x} = \frac{\partial f}{\partial X}\frac{dX}{dx} \rightarrow \frac{\partial f}{\partial x}\left(\frac{dX}{dx}\right)^{-1} = \frac{\partial f}{\partial X} \tag{5}$$

Where x is the coordinate on the non-uniform mesh and X the coordinate on the uniform mesh. A known analytical function is used for X so that the dX/dx can be calculated exactly. The restriction on the transformation given by equation (5) is that dX/dx should not become zero inside the computational domain.

We have chosen for a staggered grid in which the scalar variables are located in the center of the cell and vector quantities on the cell faces. This is illustrated in Figure 1. where we show a grid cell in 2D. The actual discretization is of course performed in three dimensions. The arrangement of the variables is similar to the one used by Harlow and Welch [3] in their classical paper. The staggered arrangement of course leads to some additional work. For instance, if we want to calculate $\partial\rho u/\partial x$ in equation (1) we first have to interpolate the density, which is a scalar and therefore located at the cell center, to the face of the cell. With the interpolated value of the density we can form the product ρu. Subsequently we can calculate the derivate $\partial\rho u/\partial x$ at the cell face and interpolate the result to the center of the cell or we can try to evaluate the derivative directly at the center of the cell using information on the faces. The latter is what we will do in the present study. The equations are integrated in time with a standard fourth order Runga-Kutta method.

[1]For conservation of mass we can use a model of the form

$$subgrid = (C_\rho\Delta)^2\frac{\partial\rho}{\partial x_i}\frac{\partial u_i}{\partial x_i}$$

For conservation of energy

$$subgrid = \overline{\rho}(C_T\Delta)^2\frac{\partial T}{\partial x_i}\frac{\partial u_i}{\partial x_i}$$

and for the mixture fraction

$$subgrid = \overline{\rho}(C_Z\Delta)^2\frac{\partial Z}{\partial x_i}\frac{\partial u_i}{\partial x_i}$$

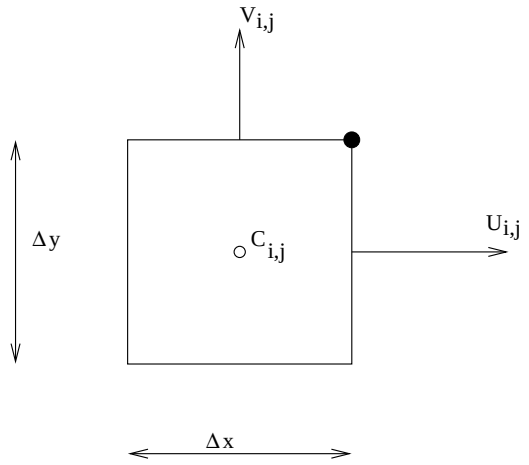

Figure 1: A two dimensional cell of the computational grid. The actual discretization is performed in three dimensions.

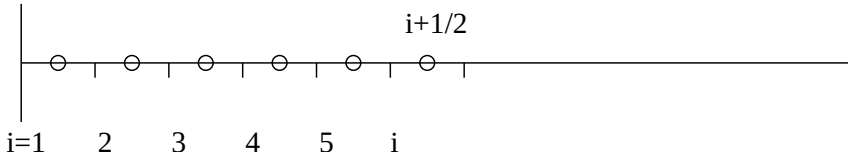

Figure 2: The distribution of the grid points.

2.1 The derivative

In the governing equations (1)-(4) and the mapping, equation (5) only first order derivatives appear. So we only have to consider a formula for the first derivative. The first derivative will always be evaluated on a staggered uniform grid as is shown in Figure 2. If the variables are known at points $i+1/2, i+3/2..$ we can use the following formula to calculate the derivatives at the points $i, i+1, ...$

$$\begin{aligned} a(f'_{i+1} + f'_{i-1}) + f'_i &= \frac{b}{\Delta X}(f_{i+1/2} - f_{i-1/2}) + \frac{c}{\Delta X}(f_{i+3/2} - f_{i-3/2}) + \\ &\quad \frac{d}{\Delta X}(f_{i+5/2} - f_{i-5/2}) + \frac{e}{\Delta X}(f_{i+7/2} - f_{i-7/2}) \end{aligned} \tag{6}$$

In which f'_i is derivative of f with respect to X in point i and ΔX is the (uniform) grid spacing. The coefficients in the equation above are obtained by Taylor expansions around grid point i. With the five coefficients a, b, c, d and e in equation (6) we can obtain an 10th order accurate formulation. The values for a, b, c, d and e for this 10th order scheme are (obtained with the Maple Software package):

$$a = 49/190,\ b = 12985/14592,\ c = 78841/364800,\ d = -343/72960,\ e = 129/851200$$

This formula can only be used far away from the boundaries. Closer to the boundaries we have to make the stencil smaller, i.e. $e = 0$. The coefficients for the resulting 8th order scheme read:

$$a = 25/118, b = 2675/2832, c = 925/5664, d = -16/28320, e = 0$$

Even closer to the boundary we have to use the 6th and 4th order formulation

$$a = 9/62, b = 63/62, c = 17/186, d = 0, e = 0, O(\Delta X^6)$$

$$a = 1/22, b = 12/11, c = 0, d = 0, e = 0, O(\Delta X^4)$$

At the boundary itself we use a one sided 3rd order accurate formulation

$$f'_i + 23f'_{i+1} = \frac{1}{\Delta X}\left(-25f_{i+1/2} + 26f_{i+3/2} - f_{i+5/2}\right)$$

The approximations above lead to a tridiagonal system with can be inverted easily and efficiently.

In the derivation of equation (6) we assumed that the variable was known in between the points i and $i+1$. In the case that the variables are known on the nodes i and that we want to know the derivative at point $i+1/2$ we can use the same formula but we have to shift the data over half a grid cell and we have to solve for $n-1$ instead of n grid points.

2.2 Interpolation and extrapolation

Apart from the relation for the first derivative we need also an interpolation procedure to interpolate variables from the locations i to locations $i+1/2$ and visa-versa. This should preferably be done with a method which has the same formal accuracy as the method which is used to obtain the derivatives. Here we consider the following compact interpolation rule

$$\begin{aligned} f_i + a(f_{i+1} + f_{i-1}) &= b(f_{i+1/2} + f_{i-1/2}) + c(f_{i_3/2} + f_{i-3/2}) + \\ &\quad d(f_{i+5/2} + f_{i-5/2}) + e(f_{i+7/2} + f_{i-7/2}) \end{aligned} \tag{7}$$

In the interior we require again 10th order accuracy resulting in the following values for the coefficients a, b, c, d and e (again obtained with the Maple Software package):

$$a = 7/18, b = 1225/1536, c = 49/512, d = -7/1536, e = 1/4608$$

Closer to the boundaries the stencil has to be made smaller, i.e. $e = 0$:

$$a = 5/14, b = 25/32, c = 5/64, d = -1/448, e = 0, O(\Delta X^8)$$

Even closer to the boundary we have to use 6th an 4th order schemes, i.e.

$$a = 3/10, b = 3/4, c = 1/20, d = 0, e = 0, O(\Delta X^6)$$

$$a = 1/6, b = 2/3, O(\Delta X^4)$$

At the boundary we use again a one sided 3rd order accurate formulation (actually this is an extrapolation instead of an interpolation):

$$f_i = 15/8 f_{i+1/2} - 5/4 f_{i+3/2} + 3/8 f_{i+5/2}$$

The formulas above results in a tridiagonal system which can be inverted easily. Again we can use the same rule to interpolate from points f_i to points $f_{i+1/2}$ by shifting the data over half a grid cell and evaluating for $n-1$ instead of n points.

The mapping, given by equation (6) takes care of the effect of the non-uniform grid on the derivatives. For the function f itself we can not use such a mapping. Formally we could construct an interpolation rule for non-uniform grids. In which the difference in grid-spacings between points $i, i-1$ and $i, i+1$ are taken into account. However, in the literature it is shown, see e.g. [7], that which such a non-uniform interpolation the kinetic energy $\rho u_i u_i/2$ is not conserved numerically. [7] shows that only with a uniform (symmetric) interpolation kinetic energy is conserved. Conservation of kinetic energy is a good start for a stable numerical solution.

Therefore, we use the interpolation rule (7) also on non-uniform grids. Formally, this will reduce the local truncation error of the scheme. However, this is the only way to strictly satisfy conservation of kinetic energy on a computational grid, see e.g. [7].

3 Advection test

In this section we will show some results of a simple advection test. The numerics given above are used to discretize the following equation:

$$\frac{\partial Z}{\partial t} - u_i \frac{\partial Z}{\partial x_i} = 0, \;\; u_i = (1, 1, 0) \tag{8}$$

At time $t = 0$ the initial condition of Z is given by the following relation:

$$Z(x_i, t) = \frac{1}{2}\left[1 - \tanh\left(\frac{5}{2}(r-2)\right)\right], \;\; r = \sqrt{[(x-4)^2 + (y+1)^2 + z]} \tag{9}$$

We have integrated equation (8) from $t = 0$ to $= 4$ on three strongly nonuniform grids with 48^3, 96^3 and 128^3 points. The coarse grid with 48^3 points is shown in Figure 3 (later we will use the same grid for some jet calculations). The initial conditions, given by equation (9) are between 0 and 1. Equation (8) has no source term so if the numerical resolution would be sufficiently fine the final solution should also have values in between 0 and 1, i.e. a pure translation of the initial condition. In Figures 4a and 4b we show the initial and final distribution of Z on the course and on the fine grid. Obviously the fine grid result is much better. However, considering the low number of grid points for the course grid case, the result is acceptable. In table 1 we have listed the minimum and maximum values of the mixture fraction when it reaches its final position. Results are included for

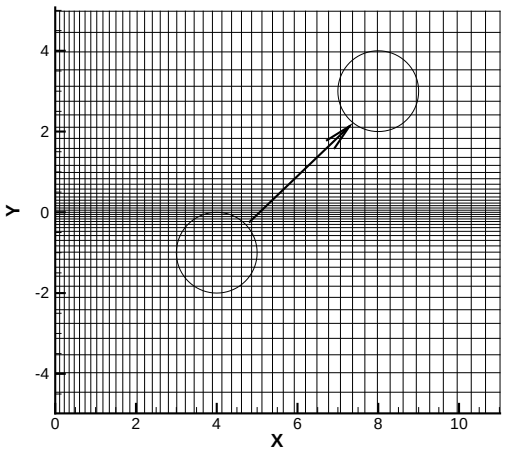

Figure 3: The computational grid with the initial and final location of the profile of the mixture fraction Z

order	48^3	96^3	128^3
6th	-0.069 , + 1.181	-0.051, + 1.071	-0.038,+1.042
8th	-0.076 , + 1.141	-0,045, + 1.048	-0.029,+1.028
10th	-0.081 , + 1.105	-0.042, + 1.039	-0.017,+1.022
12th	-0.081 , + 1.101	-0.036, + 1.037	-0.011,+1.015
exact	0 , +1	0, +1	0, +1

Table 1: The minimum and maximum value of Z at time $t = 4$ for three different mesh sizes and four different orders of the spatial discretization.

three different grid size and 4 different orders of the numerical method. Increasing the order of the scheme or the number of grid points gives better results. Note that the main cost of the scheme is associated with inverting the matrix system. Therefore, increasing the order from 6th to 12th order does not significantly increase the CPU time.

4 Results for a simple jet flow

In this section we will show some results obtained from the solution of the Large Eddy equations, for the case of a round jet. The Reynolds number of the jet based on jet nozzle quantities is equal to 4,000 and the Mach number based on nozzle conditions is equal to 0.7. The grid consists of $128 \times 96 \times 96$ points in the streamwize and crossstream directions respectively. The values of the constants in the subgrid model are all set to 0.08. It should be noted that no significant difference in the results was observed for zero values of the coefficients. This is probably due to the rather low Reynolds number of the flow.

In Figure 5 we show the contours of the fluid vorticity and the computational grid. The

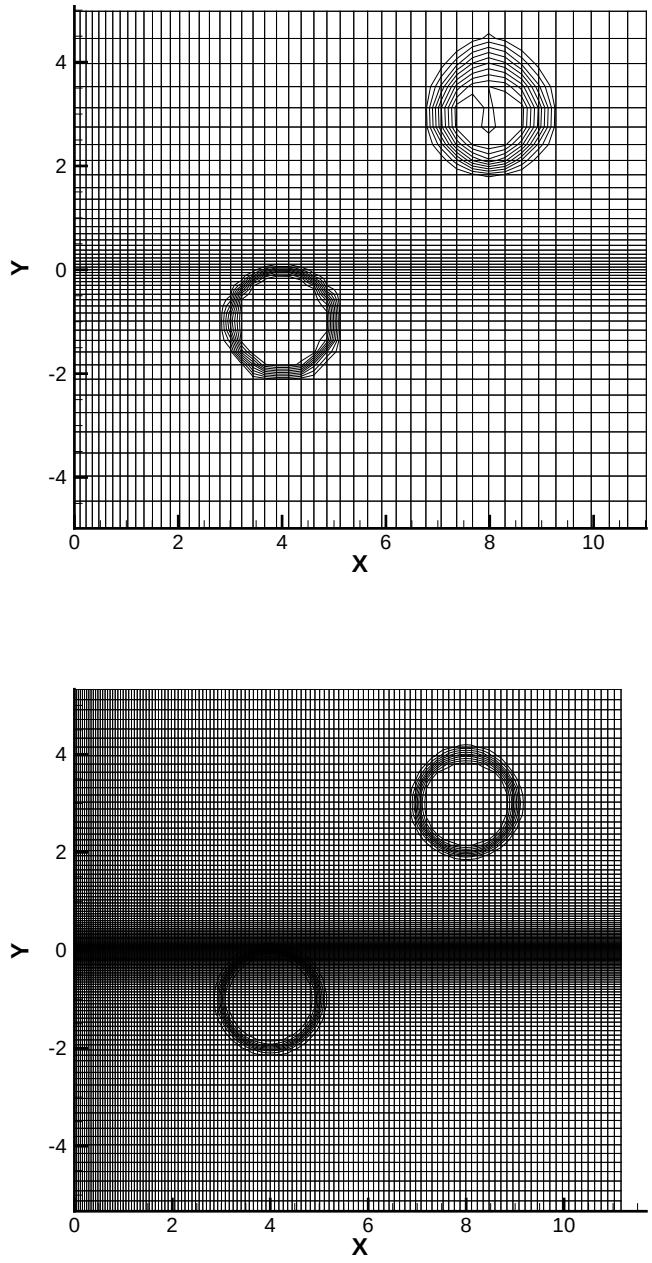

Figure 4: The initial and final position of the mixture fraction Z. Top figure, course mesh with 48^3 points, bottom figure fine mesh with 128^3 grid points.

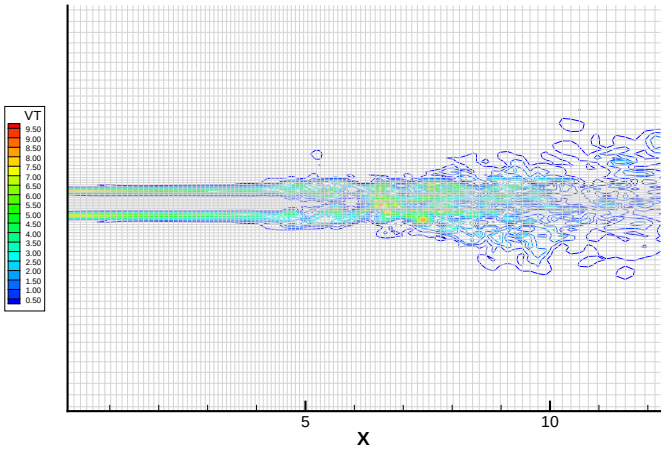

Figure 5: The magnitude of the vorticity vector in a round turbulent jet with a Reynolds number of 4,000 and a Mach number of 0.7

jet is entering the fluid domain with a laminar velocity profile as given by Michalke [6] a few diameters downstream of the jet nozzle the Kelvin-Helmholtz type of instabilities start to developed, eventually leading to a fully three dimensional flow far downstream of the jet nozzle. In Figure 6 we show the density obtained from the Large Eddy Simulations. Due to turbulent dissipation in the shear-layer the jet is slightly heated and as a result the density in the jet is a bit smaller than the ambient density. In Figure 7 we show the mixture fraction Z in the turbulent jet. The mixture fraction is bounded between 0 and 1.

5 Conclusion

In this paper we have presented a high order staggered compact finite difference method. In the interior of the domain this method has a very high order of accuracy, up to 12. The advantage of this method over standard compact finite difference methods is its increased numerical stability. For scalar transport the method is not strictly monotonic, i.e. small negative values of the scalars can occur, due to a too low numerical resolution. The standard approach would be to use a scheme with a flux limiter, for instance the well known scheme by van Leer [4]. The disadvantage of these schemes that they add a lot of dissipation in areas with sharp gradients. The turbulence model is also adding dissipation to the system. With the present approach only the dissipation provided by the turbulence model is sufficient.

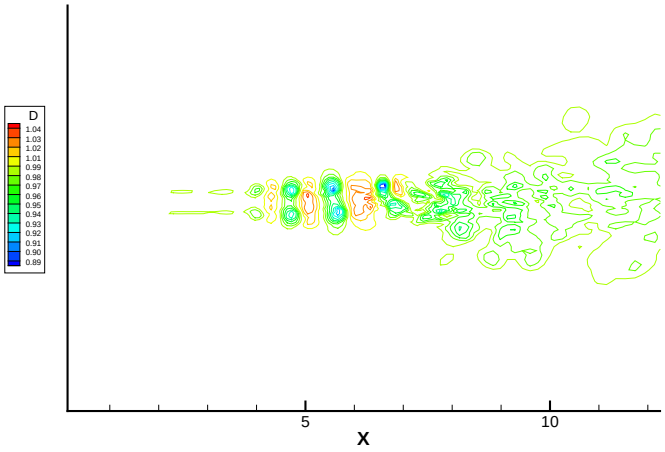

Figure 6: The density distribution in a round turbulent jet with a Reynolds number of 4,000 and a Mach number of 0.7.

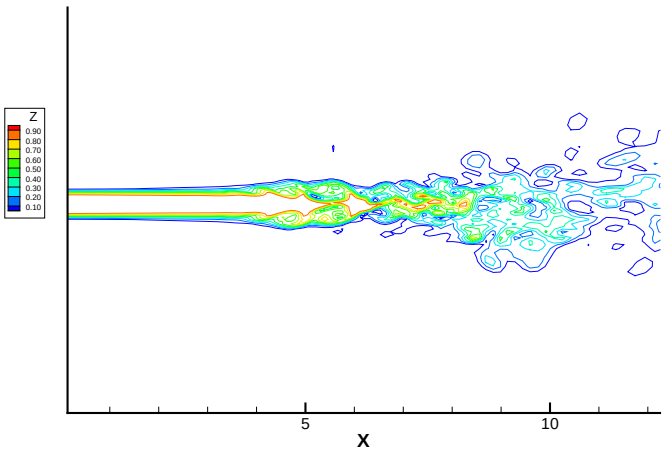

Figure 7: The mixture fraction Z in a round turbulent jet.

REFERENCES

[1] Boersma, B.J., 2005, A staggered compact finite difference approach for the Compressible Navier-Stokes equations, *J. of Comp. Phys*, **208**, 675-690.

[2] Chu, P., & Fan, C., 1998, A three point combined compact difference scheme,*J. Comp. Phys.*, **140**, 370.

[3] Harlow, F.H., & Welch, J.E., 1965, Numerical calculation of time-dependent viscous incompressible flow of fluid with a free surface, *Phys of Fluids*, **8**, 2182

[4] van Leer, B., 1977, Towards the ultimate conservative difference scheme IV. A new approach to numerical convection, *J. Comp. Phys.*, **23**, 276-299.

[5] Lele, S.K., 1992, Compact finite differences with spectral like resolution, *J. Comp. Phys.*, **103**, 16.

[6] Michalke, A., 1984, Survey on jet instability theory, *Prog. Aero. Sci.*, **21**, 159-199.

[7] Verstappen, R.W.C.P., & Veldman, A.E.P., 2003, Symmetry-preserving discretization of turbulent flow, *J. Comp. Phys.*, **187**, 343.

[8] Wilcox, D.C., 1998, Turbulence modeling for CFD, DCW Industries.